



OPEN

# Interleukin-1 $\alpha$ links peripheral Ca<sub>v</sub>2.2 channel activation to rapid adaptive increases in heat sensitivity in skin

Anne-Mary N. Salib<sup>1</sup>, Meredith J. Crane<sup>2</sup>, Sang Hun Lee<sup>3</sup>, Brian J. Wainger<sup>3</sup>,  
Amanda M. Jamieson<sup>2</sup> & Diane Lipscombe<sup>1</sup>✉

Neurons have the unique capacity to adapt output in response to changes in their environment. Within seconds, sensory nerve endings can become hypersensitive to stimuli in response to potentially damaging events. The underlying behavioral response is well studied, but several of the key signaling molecules that mediate sensory hypersensitivity remain unknown. We previously discovered that peripheral voltage-gated Ca<sub>v</sub>2.2 channels in nerve endings in skin are essential for the rapid, transient increase in sensitivity to heat, but not to mechanical stimuli, that accompanies intradermal capsaicin. Here we report that the cytokine interleukin-1 $\alpha$  (IL-1 $\alpha$ ), an alarmin, is necessary and sufficient to trigger rapid heat and mechanical hypersensitivity in skin. Of 20 cytokines screened, only IL-1 $\alpha$  was consistently detected in hind paw interstitial fluid in response to intradermal capsaicin and, similar to behavioral sensitivity to heat, IL-1 $\alpha$  levels were also dependent on peripheral Ca<sub>v</sub>2.2 channel activity. Neutralizing IL-1 $\alpha$  in skin significantly reduced capsaicin-induced changes in hind paw sensitivity to radiant heat and mechanical stimulation. Intradermal IL-1 $\alpha$  enhances behavioral responses to stimuli and, in culture, IL-1 $\alpha$  enhances the responsiveness of *Trpv1*-expressing sensory neurons. Together, our data suggest that IL-1 $\alpha$  is the key cytokine that underlies rapid and reversible neuroinflammatory responses in skin.

Sensory nerve endings in skin are highly plastic; their sensitivity to stimuli can change rapidly, and reversibly, protecting against potentially damaging insults<sup>1</sup>. Neuroinflammatory responses in skin are triggered by intense or high frequency stimulation of peripheral sensory neurons<sup>2</sup>. A critical rise in intracellular calcium in sensory neurons induces the release of inflammatory signaling molecules, including neuropeptides calcitonin gene-related peptide (CGRP), Substance P, and ATP, all of which have downstream consequences on neuroimmune signaling that underlies the cellular changes associated with inflammation and pain<sup>3–7</sup>. The generation of cytokines from immune cell activation via transmitter receptors such as P2X7, is the key step in defining the inflammatory response including its time course and the involvement of different classes of neighboring sensory nerve endings.

The rapid, adaptive increase in sensitivity to sensory stimuli in skin, in response to potentially damaging events, is one of the best-known examples of neuronal adaptation, but the molecules that mediate the initiating, early steps of the neuroinflammatory response are not fully characterized. In an earlier study, we discovered that voltage-gated Ca<sub>v</sub>2.2 channels expressed in *Trpv1*-nociceptor nerve endings are essential for initiating the rapid neuroinflammatory response to radiant heat following intradermal injection of capsaicin in mice<sup>8</sup>.

Ca<sub>v</sub>2.2 channels are abundantly expressed in sensory neurons<sup>9–11</sup>. Our lab, and others have shown that Ca<sub>v</sub>2.2 channels are expressed in sensory neurons of DRG neurons, including in small diameter, capsaicin-responsive neurons, where they contribute to the voltage-gated calcium current<sup>8,9,12–21</sup>. Immunohistochemistry and functional analyses using highly selective conotoxins has shown that Ca<sub>v</sub>2.2 channels are concentrated at a subset of presynaptic terminals in the central and peripheral nervous systems<sup>15,22–27</sup>. In sensory neurons, Ca<sub>v</sub>2.2 channels have long been known to control calcium entry at presynaptic nerve endings of primary nociceptive afferent synapses in the dorsal horn of the spinal cord<sup>28–31</sup>. Intrathecal delivery of highly specific pharmacological inhibitors of Ca<sub>v</sub>2.2 (N-type) channels are analgesic and have been used to treat otherwise intractable pain<sup>15,16,32–43</sup>.

<sup>1</sup>Department of Neuroscience, Carney Institute for Brain Science, Brown University, Providence, RI 02912, USA. <sup>2</sup>Department of Molecular Microbiology and Immunology, Brown University, Providence, RI 02912, USA. <sup>3</sup>Department of Neurology, Massachusetts General Hospital, Boston, MA 02114, USA. ✉email: Diane\_Lipscombe@brown.edu

Intrathecal  $\omega$ -CgTx MVIIA rapidly prolonged paw withdrawal latencies to both thermal and mechanical stimuli<sup>40</sup> consistent with what we observed with global  $\text{Ca}_v2.2$  KO mice (<sup>8</sup> Fig. 2). We previously showed that a local single dose of  $\omega$ -CgTx MVIIA applied intradermally reduced the robust increase in sensitivity to radiant heat that followed intradermal capsaicin, independent of  $\text{Ca}_v2.2$  channel activity at presynaptic sites in the dorsal horn of the spinal cord<sup>8</sup>. Interestingly,  $\text{Ca}_v2.2$  channel activity was not essential for the cross-sensitization of mechanoreceptors in the intradermal capsaicin model in the same animals. We also showed that inhibition of P2X7 purinergic receptors, an ATP-gated ion channel that activates immune cells to trigger the release of IL-1 inflammatory cytokines<sup>44</sup>, reduced intradermal capsaicin-induced rapid heat hypersensitivity in skin<sup>8</sup>. The cytokines that link intense activation of *Trpv1*-nociceptors to the rapid, early phase of the inflammatory response in skin, notably sensory hypersensitivity of nerve endings across sensory modalities, are incompletely characterized.

Proinflammatory cytokines such as IL-6, IL-1 $\beta$  and TNF $\alpha$ , are generated during chronic neuroinflammation in skin<sup>45–47</sup>. In addition, IL-1 $\beta$  has been shown to induce changes in excitability of neurons in culture, through effects on ion channel currents and second messenger systems<sup>1,48</sup>. These cytokines are elevated in response to prolonged neuroinflammatory conditions associated with pain, however, most studies measure cytokine levels during the later phases of inflammation, not in the initial acute phase of the rapid hypersensitivity response<sup>49,50</sup>. To address this, we extracted and analyzed interstitial fluid from mouse hind paws within 15 min following intradermal capsaicin, under conditions that result in rapid behavioral changes in skin to sensory stimuli. Intradermal capsaicin is a well-used model of adaptive sensory hypersensitivity in skin with onset and offset kinetics of tens of minutes. This model parallels short-lasting, heat-induced neuroinflammatory responses in human skin<sup>51–53</sup>.

We show that IL-1 $\alpha$ , a proinflammatory alarmin and one of the earliest immune signaling molecules, is generated locally and abundantly in interstitial fluid in response to intradermal capsaicin. The timing of elevated IL-1 $\alpha$  levels parallels peak behavioral hypersensitivity to both radiant heat and mechanical stimuli. Our data suggest that IL-1 $\alpha$  is both necessary and sufficient to trigger rapid neuroinflammation in hind paws of both *Trpv1*-nociceptors and mechanoreceptors. Our combined findings suggest that co-activation of TRPV1 receptors and voltage-gated  $\text{Ca}_v2.2$  channels are necessary to trigger the release of IL-1 $\alpha$  that may subsequently feed back on *Trpv1*-nociceptors to enhance heat responsiveness. Understanding the paracrine signaling, between sensory nerve endings and immune cells in skin during inflammation, will inform strategies to selectively target maladaptive forms of pain while leaving acute protective pain relatively intact.

## Results

Intradermal capsaicin injection induces a robust, rapid, and reversible increase in the sensitivity of the paw to both heat and mechanical stimuli. To identify the cytokines released in the hind paw in response to intradermal capsaicin, and to assess the dependency of cytokine release on global and local  $\text{Ca}_v2.2$  channel activity in skin, we recovered 7–10  $\mu\text{l}$  of interstitial fluid from both paws of each animal, 15 min post injection of capsaicin using three experimental conditions: Intradermal capsaicin in WT, in global  $\text{Ca}_v2.2^{-/-}$  KO, and in WT co-injected with  $\omega$ -CgTx MVIIA. At the 15 min time point, after capsaicin injection, behavioral responses to radiant heat and mechanical stimuli were enhanced significantly (<sup>8</sup>; Fig. 2). The  $\text{Ca}_v2.2^{-/-}$  KO mouse strain was generated in our lab and is a global deletion of  $\text{Ca}_v2.2$  (as described previously<sup>8</sup>).  $\omega$ -CgTx MIIA is a high affinity, highly selective, and slowly reversible inhibitor of voltage-gated  $\text{Ca}_v2.2$  channels<sup>33,54</sup>. We co-injected  $\omega$ -CgTx MIIA together with capsaicin to assess the contributions of peripheral voltage-gated  $\text{Ca}_v2.2$  channels in the skin, locally at the site of injection<sup>8,55,56</sup>.

### IL-1 $\alpha$ levels are elevated in interstitial fluid in hind paws in response to intradermal capsaicin

Pilot screens of 20 cytokines were performed on hind paw fluid samples from each experimental condition between two immunoassays, a multiplex bead-based immunoassay (LEGENDplex) and an electrochemiluminescence spot-based immunoassay (MSD, see “Methods” Section). Based on these results, and reports in the literature, 13 cytokines were selected as likely neuroinflammatory candidates and screened for using a custom mouse panel LEGENDplex panel. Pooled, paw fluid samples ( $n = 11–22$  mice) were screened. Of the 13 cytokines assayed, only IL-1 $\alpha$  was consistently detected in hind paw fluid under any condition at the 15 min time point in both assays. We used a second independent custom panel, Meso Scale Discovery (MSD), to validate IL-1 $\alpha$  levels in the same samples (Supplementary Fig. S1). In addition, we assessed: 8 of the same 13 cytokines surveyed on the LEGENDplex, as well as 3 cytokines that were undetectable on our pilot LEGENDplex screen, and macrophage derived chemokine (MDC) which was unique to the MSD platform (Fig. 1a).

IL-1 $\alpha$  levels were increased significantly in response to intradermal capsaicin in WT mice as compared to saline injected paws (capsaicin vs saline; two-way ANOVA with Tukey correction:  $p = 0.0002$ ; Fig. 1b). The IL-1 $\alpha$  response to capsaicin was reduced, but not eliminated, in  $\text{Ca}_v2.2^{-/-}$  global KO mice (Fig. 1b;  $p = 0.0158$ ) and also in WT mice co-injected with  $\omega$ -CgTx MVIIA (Fig. 1b;  $p = 0.0025$ ), as compared to samples from WT hind paws. We compared the IL-1 $\alpha$  levels in hind paws of capsaicin-injected  $\text{Ca}_v2.2^{-/-}$  and WT mice co-injected with  $\omega$ -CgTx MVIIA mice and these were similar to levels in control hind paws injected with saline (Fig. 1b).

To control for the possible involvement of systemic differences in IL-1 $\alpha$  levels across mice under different experimental conditions, we measured IL-1 $\alpha$  in serum of the same experimental animals. IL-1 $\alpha$  levels in serum were much lower than those at the site of capsaicin injection and they were unaffected by intradermal capsaicin (Fig. 1c). We consistently detected low levels of two cytokines in addition to IL-1 $\alpha$  in serum samples, CXCL10 and CCL5, and the levels of these cytokines were not correlated with intradermal capsaicin injection.

In a complementary approach, we measured IL-1 $\alpha$  levels using single analyte ELISA levels in hind paw skin-conditioned media. We harvested skin from hind paws of WT mice 5 min after intradermal capsaicin (ipsilateral) and saline (contralateral) injection. IL-1 $\alpha$  levels in hind paw skin-conditioned media from capsaicin injected paws

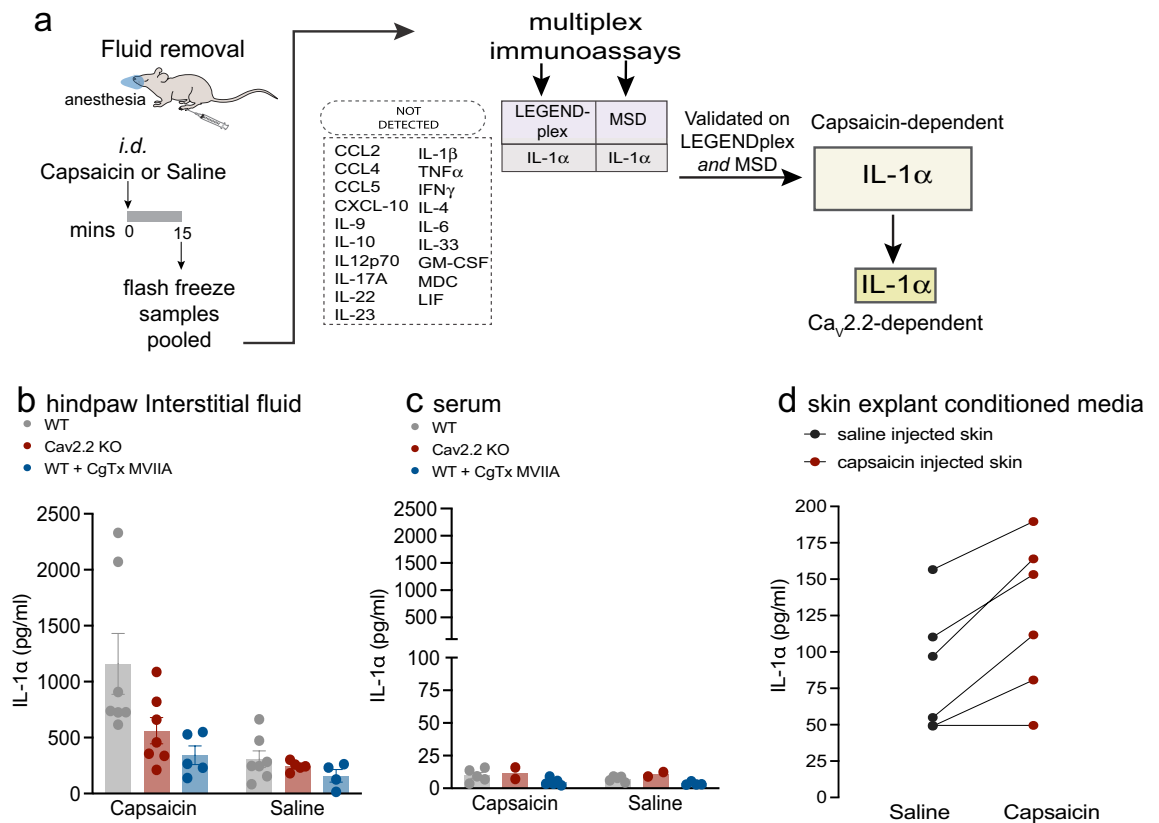


**Figure 1.** The cytokine IL-1 $\alpha$  is present in paw interstitial fluid and its levels increase with intradermal capsaicin and local Ca $_v$ 2.2 channel activity. **a.** Experimental procedures and cytokines screened are shown. Interstitial fluid extracted 15 min following 50  $\mu$ l intradermal injection in both paws of 0.1% w/v capsaicin, saline, 0.1% w/v capsaicin with 2  $\mu$ M  $\omega$ -conotoxin MVIIA, or saline with 2  $\mu$ M  $\omega$ -conotoxin MVIIA. Pooled samples were screened for 20 cytokines listed. **b.** IL-1 $\alpha$  levels in hind paw fluid based on panel standards, detected using an inflammatory multiplex bead-based immunoassay (BioLegend, LEGENDplex). Individual points represent pooled samples from wild-type (WT, gray), Ca $_v$ 2.2 $^{-/-}$  (KO, red), and WT co-injected with  $\omega$ -conotoxin MVIIA (CgTx-MVIIA, blue). Number of (pooled samples/mice) for WT with saline (7/18); KO with saline (5/11); WT with capsaicin (7/20); KO with saline (7/17); WT with capsaicin + CgTx-MVIIA (5/14); WT saline with CgTx-MVIIA (4/12). Bars represent the mean for each condition. Mean  $\pm$  SE for capsaicin: WT = 1159  $\pm$  272 pg/ml; KO = 561  $\pm$  117 pg/ml; WT + CgTx MVIIA = 343  $\pm$  83 pg/ml. *p*-values calculated by two-way ANOVA with Tukey HSD correction for multiple comparisons hind paw fluid WT capsaicin|WT saline: *p* = 0.0002; KO capsaicin|KO saline: *p* = 0.1600; WT CgTx-MVIIA + capsaicin|WT CgTx-MVIIA + saline: *p* = 0.4732. WT capsaicin|KO capsaicin: *p* = 0.0158; WT capsaicin|WT CgTx-MVIIA + capsaicin: *p* = 0.0025; KO capsaicin|WT CgTx-MVIIA + capsaicin: *p* = 0.5875. **c.** IL-1 $\alpha$  levels in serum detected using the same cytokine screening protocol as in Fig. 1b. Individual points represent pooled samples from the same animals used for hind paw fluid analysis. Bars represent the mean for each condition. Analysis of variance interaction between Injection|Genotype was measured by two-way ANOVA: *p* = 0.8422. **(d)** IL-1 $\alpha$  levels in skin-explant conditioned media detected using a single analyte ELISA (*n* = 6). Skin punch biopsies were removed 5 min post-injection and placed in media for 5 min. Each mouse was injected with saline in one paw and capsaicin in the other for within-animal comparison. Average skin weight for capsaicin injected skin: 5.48 mg; saline injected skin: 4.82 mg. Points represent analysis of conditioned media from each paw and solid lines connect saline and capsaicin injected paws for each mouse; *p*-value calculated by paired t-test: *p* = 0.0099.

were significantly higher, as compared to those from saline injected hind paws (5 of 6 mice; Fig. 1d; *p* = 0.0099, paired t-test). Collectively, our data show that intradermal capsaicin triggers IL-1 $\alpha$  release in hind paws within the first 5 min of injection, paralleling the rapid time course of behavioral changes in hind paw sensitivities to heat and mechanical stimuli (Fig. 2).

### IL-1 $\alpha$ is necessary for the development of capsaicin-induced increases in sensitivity to heat and mechanical stimuli

To establish if IL-1 $\alpha$  levels are increased *and* necessary for capsaicin-induced changes in hind paw sensitivity to heat, we co-injected a specific neutralizing monoclonal IL-1 $\alpha$  antibody (anti-mIL-1 $\alpha$ -IgG, InvivoGen, Catalog # mabg-mil1a) to occlude its actions locally, at the same site of capsaicin injection. We measured hind paw sensitivity to radiant heat and mechanical stimuli in WT mice following capsaicin injection in the absence, and

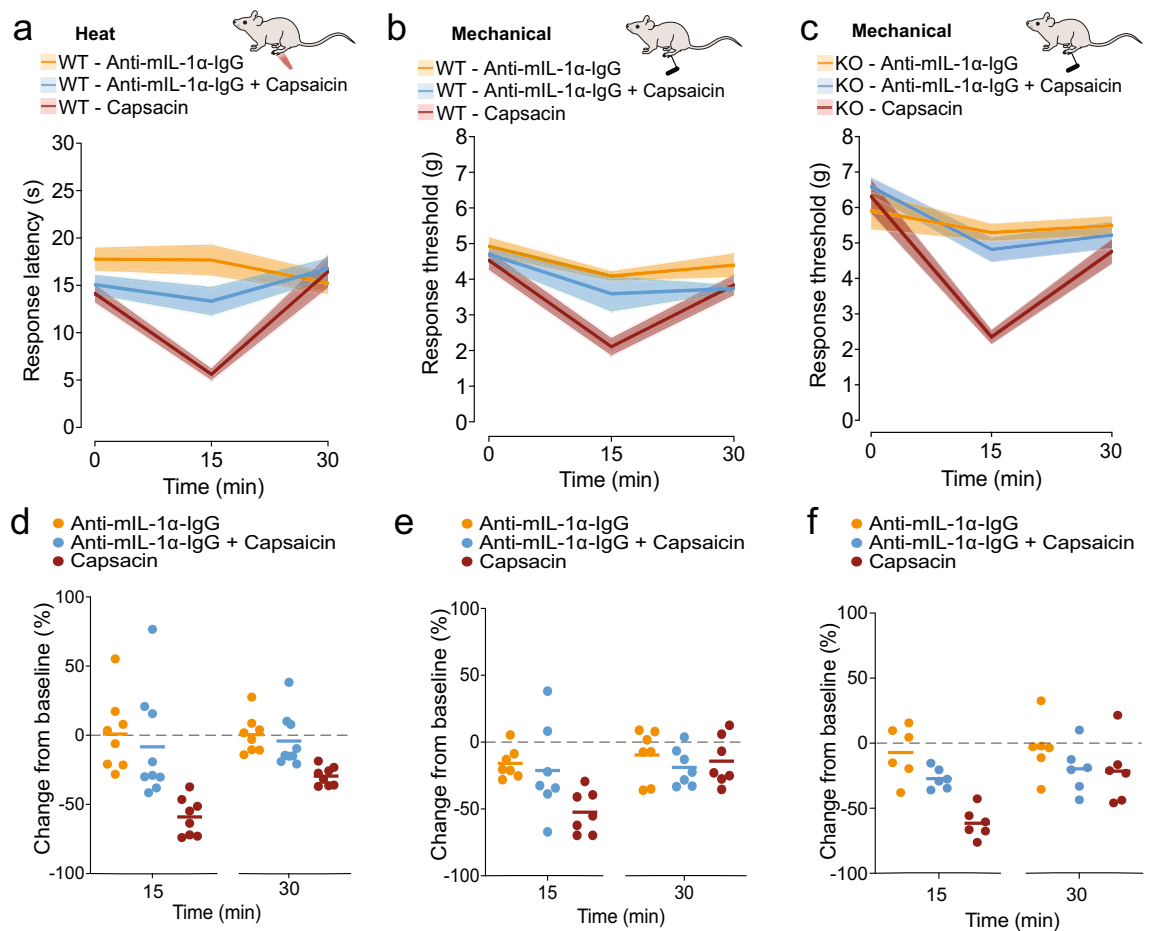


**Figure 2.** Neutralizing IL-1 $\alpha$  in the presence of capsaicin reduces both heat and mechanical hypersensitivity. Paw withdrawal response latencies to radiant heat (**a, d**) and mechanical force (g) using automated Von Frey filament (**b–c, e–f**) represented as mean values (lines)  $\pm$  SE (shaded area) (*top; a,b,c*) and average responses for individual mice (solid circles) and average values for all mice (horizontal line) represented as percent change from baseline (0 min) (*bottom; d,e,f*). Measurements were made immediately prior to (0), and 15 and 30 min post intradermal (*id*) injections as noted. (**a,d**) WT ( $Ca_v2.2^{+/+}$ ) mice received 20  $\mu$ l *id* of: 1  $\mu$ g/ml Anti-mIL-1 $\alpha$ -IgG (orange; n = 8); 0.1% w/v capsaicin + 1  $\mu$ g/ml Anti-mIL-1 $\alpha$ -IgG (blue; n = 9); 0.1% w/v capsaicin (red; n = 8). Mean  $\pm$  SE latencies to heat at 15 min: 1  $\mu$ g/ml Anti-mIL-1 $\alpha$ -IgG = 17.7  $\pm$  1.6 s; 0.1% w/v capsaicin + 1  $\mu$ g/ml Anti-mIL-1 $\alpha$ -IgG = 13.3  $\pm$  1.5 s; 0.1% w/v capsaicin = 5.6  $\pm$  0.6 s. (**d**) 15 min post: capsaicin + 1  $\mu$ g/ml Anti-mIL-1 $\alpha$ -IgG (blue) = -8.35  $\pm$  12.97%; capsaicin = -59.08  $\pm$  4.84%; Anti-mIL-1 $\alpha$ -IgG (orange) = 0.88  $\pm$  9.58%. Type|Time interaction  $p$  = 0.0008; at 15 min post *id* for: Capsaicin + 1  $\mu$ g/ml Anti-mIL-1 $\alpha$ -IgG|Capsaicin:  $p$  = 0.0001; Capsaicin + Anti-mIL-1 $\alpha$ -IgG|Anti-mIL-1 $\alpha$ -IgG  $p$  = 0.6887. (**b,e**) WT ( $Ca_v2.2^{+/+}$ ) mice received 20  $\mu$ l *id* of: 1  $\mu$ g/ml Anti-mIL-1 $\alpha$ -IgG (orange, n = 7); 0.1% w/v capsaicin + 1  $\mu$ g/ml Anti-mIL-1 $\alpha$ -IgG (blue, n = 7); 0.1% w/v capsaicin (red, n = 7). Mean  $\pm$  SE mechanical response threshold at 15 min: 1  $\mu$ g/ml Anti-mIL-1 $\alpha$ -IgG = 4.09  $\pm$  0.13 g; 0.1% w/v capsaicin + 1  $\mu$ g/ml Anti-mIL-1 $\alpha$ -IgG = 3.59  $\pm$  0.49 g; 0.1% w/v capsaicin = 2.10  $\pm$  0.24 g. **e.** 15 min post: capsaicin + 1  $\mu$ g/ml Anti-mIL-1 $\alpha$ -IgG (blue) = -21.23  $\pm$  13.00%; capsaicin = -52.40  $\pm$  6.04%, 1  $\mu$ g/ml Anti-mIL-1 $\alpha$ -IgG (orange) = -15.90  $\pm$  4.36%. Injection Type|Time interaction:  $p$  = 0.0101; 15 min post *id* for: capsaicin + 1  $\mu$ g/ml Anti-mIL-1 $\alpha$ -IgG | Capsaicin:  $p$  = 0.0179; capsaicin + Anti-mIL-1 $\alpha$ -IgG|Anti-mIL-1 $\alpha$ -IgG  $p$  = 0.8753. (**c,f**) KO ( $Ca_v2.2^{-/-}$ ) mice received 20  $\mu$ l *id* of: 1  $\mu$ g/ml Anti-mIL-1 $\alpha$ -IgG (orange, n = 6); 0.1% w/v capsaicin + 1  $\mu$ g/ml Anti-mIL-1 $\alpha$ -IgG (blue, n = 6); 0.1% w/v capsaicin (red, n = 6). Mean  $\pm$  SE mechanical response threshold at 15 min: 1  $\mu$ g/ml Anti-mIL-1 $\alpha$ -IgG = 5.29  $\pm$  0.25 g; 0.1% w/v capsaicin + 1  $\mu$ g/ml Anti-mIL-1 $\alpha$ -IgG = 4.82  $\pm$  0.35 g; 0.1% w/v capsaicin = 2.35  $\pm$  0.20 g. Analysis of variance measured by two-way ANOVA and Tukey's HSD correction for multiple comparisons. (**f**) 15 min post: capsaicin + 1  $\mu$ g/ml Anti-mIL-1 $\alpha$ -IgG (blue) = -27.22  $\pm$  3.27%; capsaicin = 61.52  $\pm$  4.70%, 1  $\mu$ g/ml Anti-mIL-1 $\alpha$ -IgG (orange) = -7.13  $\pm$  8.38%. Injection Type|Time interaction:  $p$  = 0.0175; 15 min post *id* for: capsaicin + 1  $\mu$ g/ml Anti-mIL-1 $\alpha$ -IgG|Capsaicin:  $p$  = 0.0081; capsaicin + Anti-mIL-1 $\alpha$ -IgG|Anti-mIL-1 $\alpha$ -IgG  $p$  = 0.1579.

in the presence of anti-mIL-1 $\alpha$ -IgG (Fig. 2). Baseline behavioral responses to heat and mechanical stimuli were not consistently affected by anti-mIL-1 $\alpha$ -IgG ruling out any direct effect on stimulus–response pathways. By

contrast, anti-mIL-1 $\alpha$ -IgG reduced significantly capsaicin-induced increases in the sensitivity of mouse hind paws to both heat ( $p = 0.008$ ) and mechanical ( $p = 0.012$ ) stimuli (Fig. 2a–e).

In a previous study, we showed that Ca $_v$ 2.2 channel activity was essential for capsaicin-induced hypersensitivity to heat, but notably, not mechanical stimulation, which was fully intact in Ca $_v$ 2.2 $^{-/-}$  mice and in hind paws of WT mice injected with  $\omega$ -CgTx MVIIA. IL-1 $\alpha$  levels in response to capsaicin were reduced, but not eliminated, in the Ca $_v$ 2.2 $^{-/-}$  global KO mouse (Fig. 1b). We therefore tested the hypothesis that IL-1 $\alpha$  levels were still sufficient to mediate capsaicin-induced mechanical hypersensitivity in mice lacking Ca $_v$ 2.2 channels. We used anti-mIL-1 $\alpha$ -IgG to neutralize IL-1 $\alpha$  in Ca $_v$ 2.2 $^{-/-}$  animals and showed that it significantly reduced capsaicin-induced mechanical hypersensitivity ( $p = 0.0081$ , Figure 2c,f). The use of anti-mIL-1 $\alpha$ -IgG to specifically neutralize the actions IL-1 $\alpha$  locally, establish IL-1 $\alpha$  as a critical immune signal in the capsaicin-induced neuroinflammatory response in skin.

To establish if IL-1 $\alpha$  is sufficient to induce rapid changes in the sensitivity of skin to heat and mechanical stimuli, we directly injected recombinant IL-1 $\alpha$  (mIL-1 $\alpha$ , R&D catalog #: 400-ML-005/CF) into the hind paws of mice and assessed their behavior. Paw withdrawal responses to both heat and mechanical stimuli were evoked with shorter latencies (heat) and at lower forces (mechanical) in mice injected with recombinant IL-1 $\alpha$  at 15- and 30-min time points post injection, as compared to responses of contralateral paws in the same animals (Fig. 3). Similarly, recombinant IL-1 $\alpha$  injected paws were hypersensitive to radiant heat and mechanical stimuli as compared to vehicle injected controls (PBS 10% FBS); Heat: 15 min mIL-1 $\alpha$  compared to vehicle  $p = 0.07$ , mechanical at 15 min  $p = 0.02$ . Heat: 30 min mIL-1 $\alpha$  compared to vehicle  $p = 0.005$ , mechanical at 30 min  $p = 0.056$ .

Based on our findings, we conclude that IL-1 $\alpha$  is a critical early mediator of transient heat and mechanical hypersensitivity in skin induced by capsaicin. Notably, IL-1 $\alpha$  was the only cytokine consistently detected in two different cytokine detection platforms used in our analyses. Our data also show that IL-1 $\alpha$  levels are strongly dependent on both TRPV1 receptor activation and peripheral Ca $_v$ 2.2 channel activity, suggesting that IL-1 $\alpha$  is a key immune signal underlying the rapid and robust neuroimmune response in skin to heat. Interestingly, even though capsaicin-induced hypersensitivity to mechanical stimulation is independent of Ca $_v$ 2.2 channel activity<sup>8</sup>, we show that this behavioral response also depends on IL-1 $\alpha$ .

### Overnight incubation of IL-1 $\alpha$ increases responsiveness of sensory neurons

To evaluate the impact of IL-1 $\alpha$  on nociceptor responsiveness of primary sensory neurons, we employed APPOINT (Automated Physiological Phenotyping of Individual Neuronal Types), a high-content calcium imaging platform integrating high-throughput single-cell calcium imaging, liquid handling, automated cell segmentation, and analysis including machine learning-based calls of responding cells<sup>57</sup>. Trpv1-Cre mice were crossed with floxed channel-rhodopsin-2 (ChR2)-EYFP mice and first-generation Trpv1/ChR2-EYFP mice were used for preparation of dorsal root ganglia (DRG) neurons (see methods). We isolated DRG neurons from mice expressing the blue light-sensitive ion channel ChR2 in Trpv1-positive nociceptors and identified optically responsive neurons using a red-shifted calcium indicator. The number and frequency of stimuli (light pulses) in the optogenetic rheobase assay was calibrated to cover the dynamic range of activation<sup>57</sup>. Stimulating TrpV1/ChR2-EYFP nociceptors with trains comprised of increasing numbers of 1 ms blue light pulses allows us to measure an optical rheobase, the number of stimuli pulses necessary to evoke calcium flux in individual nociceptors. DRG neurons were plated into wells overnight with saline (vehicle) or IL-1 $\alpha$  (100 ng/ml). The following day, increasing trains of 1, 5, or 10 pulses of blue light were applied to the wells, and the % of DRG neurons exhibiting suprathreshold levels of calcium flux were quantified. Compared to saline-treated control cells, a larger percentage of cells incubated overnight with IL-1 $\alpha$  (100 ng/ml) responded to optical stimulation ( $F_{1,40} = 4.27$ ;  $p = 0.045$ , two-way ANOVA) (Fig. 4a,b). A comparison of the cumulative distribution of Ca $^{2+}$  amplitudes in responsive DRG neurons revealed a slight increase in larger amplitude events in cells treated with IL-1 $\alpha$  compared to saline (Fig. 4c), but this difference did not reach statistical significance threshold ( $p = 0.182$ , two-sample Kolmogorov–Smirnov test). Overall, these data show that IL-1 $\alpha$  can act directly on sensory neurons to alter neuronal responsiveness to optical stimulation via the Interleukin-1 receptor type 1 (IL-1R1) receptor on sensory neurons, as has been shown previously for IL-1 $\beta$ <sup>48</sup>.

### Discussion

Intradermal capsaicin is used to model one of the most well-known examples of the rapid neuroinflammatory response in skin following exposure to potentially damaging stimuli<sup>51,58,59</sup>. We applied this model in mouse hind paws analyze rapidly generated cytokines in interstitial fluid in vivo and, under the same experimental conditions, to monitor behavioral responses to radiant heat and mechanical stimulation. By two independent assays, we identified IL-1 $\alpha$  as the major cytokine generated in hind paw fluid and showed it was both necessary and sufficient to support the rapid increase in sensitivity of peripheral nerve endings in skin to sensory stimuli.

We were initially surprised that IL-1 $\alpha$  was the only cytokine identified in both cytokine screening platforms and consistently present in mouse hind paw fluid. IL-1 $\alpha$  levels were elevated within 15 min of intradermal capsaicin exposure, coincident with robust behavioral changes to both radiant heat and mechanical stimuli. Levels of IL-1 $\alpha$  measured in hind paw interstitial fluid were 3–fourfold higher following capsaicin injection in WT fluid when compared to the dynamic range of IL-1 $\alpha$  found in blood in non-injured states<sup>60</sup>. We did not consistently detect other inflammatory cytokines in interstitial fluid samples at the 15 min time point, when behavioral responses are maximal. Importantly, in both assays, we confirmed that IL-6, IL-1 $\beta$ , and TNF $\alpha$  and all other cytokines included in the screen, were detectable in concurrently run standards (Supplementary Fig. S2, Supplementary File S3).

However, our data are consistent with the known role of IL-1 $\alpha$ , an alarmin, as one of the earliest signaling molecules of the inflammatory response<sup>61</sup>. In fluid samples of human blisters, IL-1 $\alpha$ , not IL-1 $\beta$ , levels are

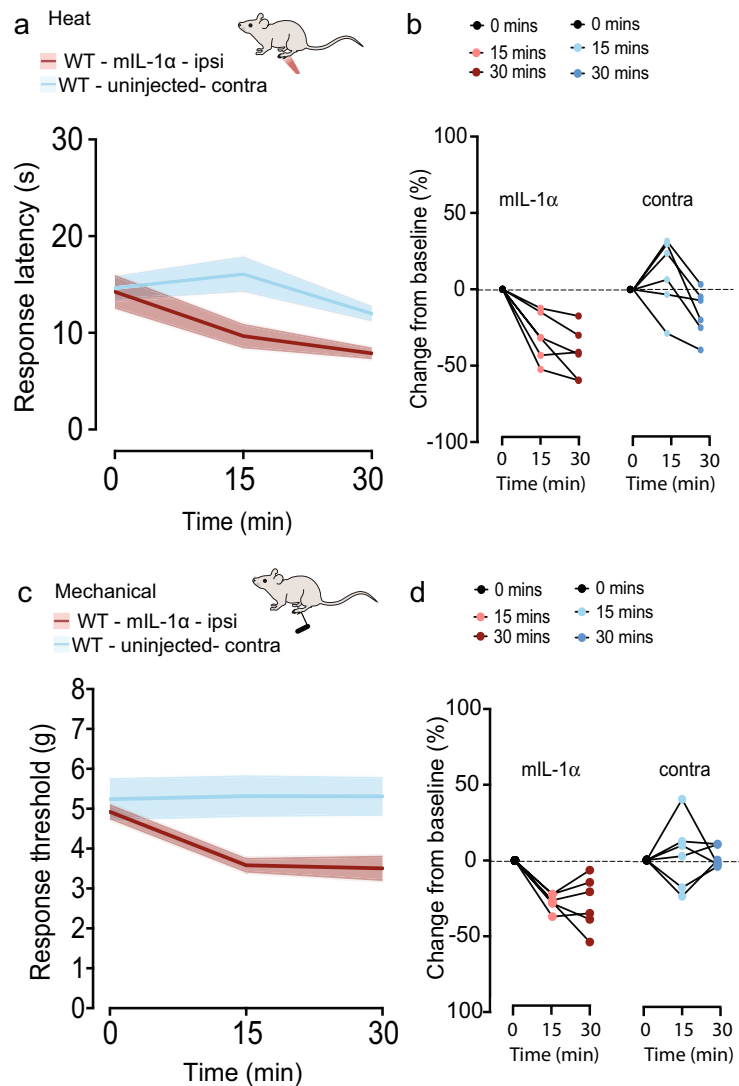


**Figure 3.** Intradermal recombinant IL-1 $\alpha$  triggers both heat and mechanical hypersensitivity in the absence of capsaicin (a). Response latency (s) to radiant heat measured before (0) and 15 and 30 min after 20  $\mu$ g/ml injection of 5  $\mu$ g/ml recombinant mouse IL-1 $\alpha$  (m-IL-1 $\alpha$ ) in sterile PBS + 10% FBS (n = 6). Injected and un-injected paws (blue). Mean  $\pm$  SE response latencies to heat 15 min following injection to: m-IL-1 $\alpha$ :  $9.66 \pm 1.26$  s and un-injected  $16.06 \pm 1.84$  s. (b) Percentage change from baseline for Individual mice in response to m-IL-1 $\alpha$  (15 min)  $-31.03 \pm 6.36\%$  and un-injected paws  $10.54 \pm 10.06\%$ . Paw injection| time interaction analysis of variance measured by two-way ANOVA and Tukey's HSD correction for multiple comparisons  $p = 0.0018$ . m-IL-1 $\alpha$  injected|un-injected  $p = 0.0075$  (15 min) and m-IL-1 $\alpha$  injected|un-injected (30 min)  $p = 0.0235$ . (c) Mean  $\pm$  SE paw withdrawal thresholds to mechanical stimuli before (0) and 15 and 30 min after 20  $\mu$ L injection of 5  $\mu$ g/ml recombinant mouse IL-1 $\alpha$  (m-IL-1 $\alpha$ ) in sterile PBS + 10% FBS (n = 6 mice). Mean  $\pm$  SE for m-IL-1 $\alpha$ :  $3.58 \pm 0.18$  g and un-injected =  $5.32 \pm 0.52$  g. (d) Average percent change from baseline for each animal at indicated time points. Mean  $\pm$  SE values at 15 min were m-IL-1 $\alpha$  =  $-27.25 \pm 2.22\%$  and un-injected =  $3.78 \pm 9.42\%$ . Paw injection| time interaction analysis of variance measured by two-way ANOVA and Tukey's HSD correction for multiple comparisons  $p = 0.0063$ . At 15 min m-IL-1 $\alpha$  injected|un-injected  $p = 0.0205$ ; 30 min m-IL-1 $\alpha$  injected|un-injected  $p = 0.0068$ .

elevated<sup>62,63</sup>. IL-1 $\alpha$  is primed and ready in skin resident immune cells for rapid action and, unlike IL-1 $\beta$  which is only biologically active in its cleaved mature form<sup>64–66</sup>, IL-1 $\alpha$  activates IL-1R1 in both its cleaved mature and precursor pro forms<sup>64</sup>. The known kinetics of IL-1 $\alpha$  are faster than IL-1 $\beta$  following stimulation. Others have shown that on the timescale of hours, IL-1 $\alpha$  is maximal within 6 h of stimulation, while IL-1 $\beta$  is maximal 12–16 h after stimulation<sup>67</sup>.

We took a number of steps to validate our findings including: (i) Employing two independent cytokine detection platforms, Custom Mouse Panel LEGENDplex and MSD U-Plex and R-plex, designed to identify low levels of cytokines in low volume fluid samples; (ii) Screening 20 different cytokines; (iii) Using single analyte

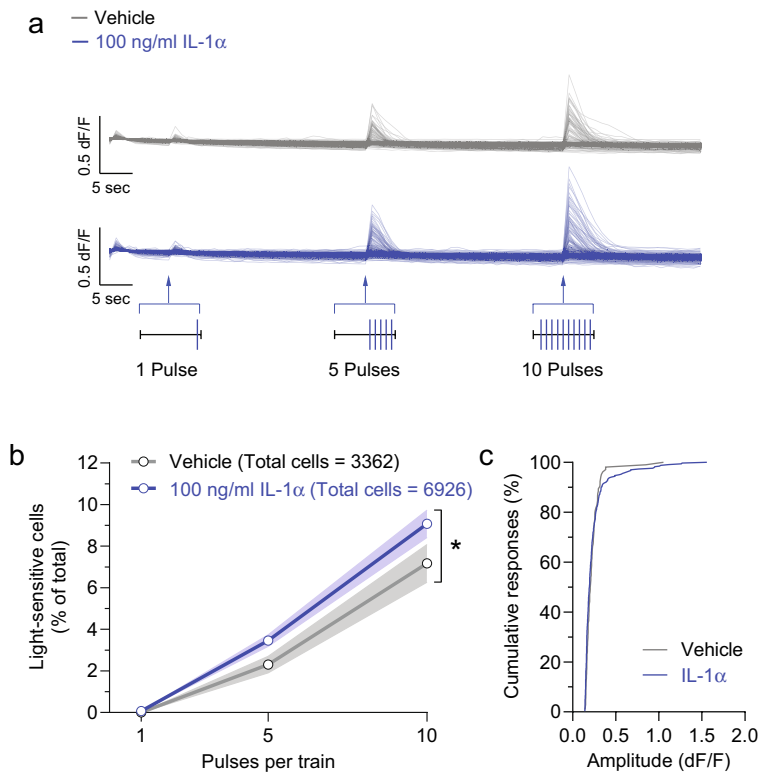


**Figure 4.** IL-1 $\alpha$  reduces the optical rheobase of Trpv1/Chr2-EYFP mouse nociceptors. **(a)** Traces of Ca<sup>2+</sup> responses evoked by blue light stimulations (trains of 1, 5, and 10 pulses of 1 ms duration). Scale bars: 5 s, 0.5 dF/F. **(b)** Averaged percentage of sensory neurons activated by increasing pulse number of blue light stimulations following treatment with vehicle and IL-1 $\alpha$  (blue: 100 ng/ml IL-1 $\alpha$ ). Note that overnight incubation with IL-1 $\alpha$  significantly increased the percentage of calcium-responsive cells compared to vehicle treatment ( $F_{1,40} = 4.27$ ;  $p = 0.045$ , two-way ANOVA with Bonferroni correction for multiple comparisons). Responsive cells were defined as previously using a machine learning-based algorithm<sup>57</sup>. All data represent mean (point/line)  $\pm$  SE (shaded area). **(c)** Cumulative distributions of calcium response amplitudes measured in DRG somas in response to 100 ng/ml IL-1 $\alpha$  (blue) or saline (grey). The Kolmogorov–Smirnov test for comparing two samples did not show a significant statistical difference ( $p = 0.182$ ).

ELISA to measure IL-1 $\alpha$  in isolated skin conditioned media; and iv) Using standards to ensure that the cytokine assays are able to detect all cytokines screened, including IL-1 $\beta$  (Supplementary Fig. S2, Supplementary File S3).

To establish if IL-1 $\alpha$  is necessary for the rapid behavioral changes in sensitivity to sensory stimuli associated with intradermal capsaicin, we employed a potent neutralizing antibody anti-mIL-1 $\alpha$ -IgG. Anti-mIL-1 $\alpha$ -IgG is selective for IL-1 $\alpha$ , and it inhibits the biological activity of both precursor and mature forms of mouse IL-1 $\alpha$  (InvivoGen, Catalog # mabg-mil1a). By contrast, pharmacological inhibition of the IL-1R1 does not distinguish between IL-1 $\alpha$  and IL-1 $\beta$  as both cytokines act through the same receptor<sup>64,68,69</sup>. The neutralization of the effects of intradermal capsaicin by anti-mIL-1 $\alpha$ -IgG, combined with the demonstration that intradermal recombinant IL-1 $\alpha$  induces heat and mechanical hypersensitivity in mouse hind paw, establish IL-1 $\alpha$  as an immune signal that mediates the rapid increase in peripheral nerve ending sensitivity to heat and mechanical stimulation.

In this study, we focus on identifying the cytokine in hind paws that underlies the rapidly developing, and rapidly reversible neuroinflammatory response in skin. Many other cytokines including IL-6, IL-1 $\beta$ , and TNF $\alpha$  are critical for mediating more sustained forms of inflammation associated with chronic pain<sup>2,45–47</sup>. Our data do not exclude the possibility that other cytokines are involved in the capsaicin response in skin, but we do show that IL-1 $\alpha$  is a critical signaling molecule in this robust protective response. It is possible that IL-1 $\alpha$  has been overlooked as critical for the rapid early phase of neuroinflammation in skin because of a greater focus on chronic inflammatory models of pain, important for identifying new therapeutic targets<sup>70–72</sup>, and the use of assays that do not distinguish IL-1 $\alpha$  and IL-1 $\beta$ .

We showed previously that voltage-gated Ca<sub>v</sub>2.2 channels in peripheral nerve endings in skin play a critical role in the development of capsaicin-induced hypersensitivity to heat<sup>8</sup>. Here we show that Ca<sub>v</sub>2.2 channel activity also contributes to increased levels of IL-1 $\alpha$  in hind paw fluid in response to intradermal capsaicin. Combining our earlier studies with data presented here suggests a model in which voltage-gated Ca<sub>v</sub>2.2 channels in *Trpv1*-nociceptor nerve endings and IL-1 $\alpha$  generating immune cells may function as a signaling unit mediating rapid neuroinflammatory responses that lead to increased heat sensitivity (Fig. 5). Our data lend support to previous studies showing that Ca<sub>v</sub>2.2 channels (N-type) are involved in inflammatory and neuropathic pain responses, as well as in microglial activation and cytokine release<sup>73,74</sup>. It is possible that different classes of voltage gated

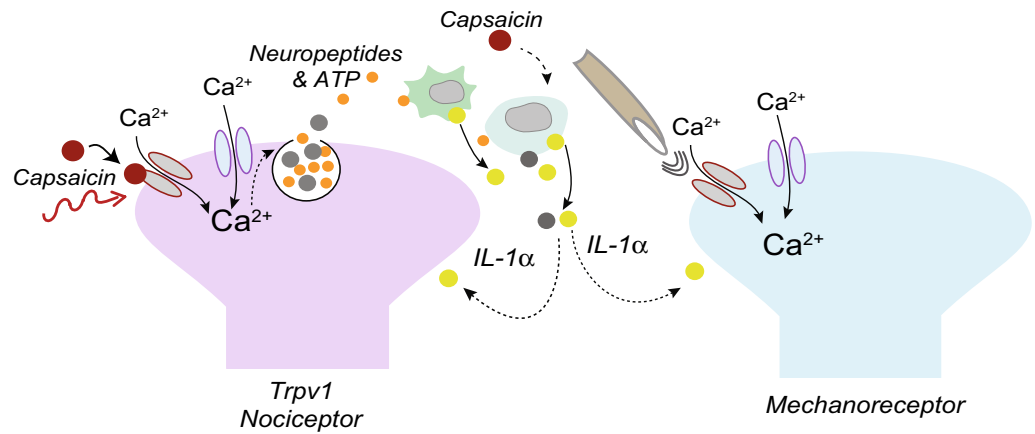


**Figure 5.** One proposed model for  $\text{Ca}_v2.2$  channel involvement in capsaicin-induced sensory hypersensitivity in skin. This model is based on combined results from published data in DuBreuil et al.<sup>8</sup> and this current report. Neuroimmune signaling underlying heat hypersensitivity involves capsaicin activation of TRPV1 receptors on *Trpv1*-expressing cells including nociceptor nerve endings in skin, which induces a membrane depolarization that triggers the opening of voltage-gated  $\text{Ca}_v2.2$  channels. Calcium enters through both  $\text{Ca}_v2.2$  channels and TRPV1 channels, and the influx of calcium through  $\text{Ca}_v2.2$  channels is critical for vesicular release of neurotransmitters. ATP is included based on our previous finding showing that the P2X7 receptor antagonist (A438079) significantly reduces capsaicin-induced heat hypersensitivity<sup>8</sup>, and ATP is known to be present in secretory vesicles<sup>10</sup>. ATP is hypothesized to bind purinergic P2X7 receptors expressed by keratinocytes and leukocytes to trigger release of IL-1 $\alpha$ . IL-1 $\alpha$  increases the sensitivity of *Trpv1*-expressing nociceptors and mechanoreceptors<sup>97</sup> to their respective stimuli in glabrous skin. Capsaicin has other targets independent of *Trpv1*-expressing sensory neurons including immune cells, that may contribute to mechanical hypersensitivity which we have shown to be independent of  $\text{Ca}_v2.2$  channel activation. These are indicated as dotted lines as further studies will be needed to dissect the mechanisms underlying capsaicin-induced hypersensitivity to mechanical stimuli.

calcium channels contribute to the generation of IL-1 $\alpha$  via mechanoreceptor activation. For example,  $\text{Ca}_v3.2$  channels (T-type), are abundant in low threshold mechanoreceptors (LTMRs)<sup>75</sup> and they have been implicated in neuroinflammatory pain signaling underlying mechanical allodynia<sup>76–78</sup>. Our conclusions and proposed model (Fig. 5) are the simplest interpretation of data presented here and on published literature: capsaicin acts on TRPV1 receptors expressed by heat responsive sensory nerve endings in skin triggering membrane depolarization, activation of  $\text{Ca}_v2.2$  channels, and release of neuropeptide and ATP that act on immune cells to trigger cytokine release (Fig. 5). But intradermal capsaicin may also act on nonneuronal *Trpv1* expressing cells in skin, including keratinocytes<sup>79</sup> T-cells<sup>80</sup> Langerhans cells<sup>81</sup> which may contribute to  $\text{Ca}_v2.2$ -independent sources of cytokines, including IL-1 $\alpha$ . For example, capsaicin could act on immune cells directly, triggering the production and/or release of IL-1 $\alpha$  independent of  $\text{Ca}_v2.2$  channels and nociceptor activation. We show that IL-1 $\alpha$  levels are significantly lower but not eliminated, in hind paw interstitial fluid when  $\text{Ca}_v2.2$  channel activity is inhibited.

The cross-sensitization of peripheral nerve endings in skin following intradermal capsaicin or naturalistic stimuli is a classic feature of the rapid protective neuroinflammatory response<sup>51,53,82–84</sup>. Our findings, using the intradermal capsaicin model of rapid inflammation, suggests that IL-1 $\alpha$  also contributes to the recruitment of different sensory modalities through a  $\text{Ca}_v2.2$  channel-independent pathway in addition to *Trpv1*-expressing nociceptors<sup>51,85</sup>. We know from our earlier studies, that capsaicin-induced mechanical hypersensitivity develops independent of peripheral  $\text{Ca}_v2.2$  channel activity in *Trpv1*-nociceptors in the same skin regions<sup>8</sup>. Anti-mIL-1 $\alpha$ -IgG occludes both heat and mechanical hypersensitivity induced by capsaicin (Fig. 2a–e), suggesting that sufficient IL-1 $\alpha$  must be generated, via a  $\text{Ca}_v2.2$  channel independent pathway, to act on mechanoreceptor nerve endings in skin (Fig. 5). We showed that neutralizing IL-1 $\alpha$  in our  $\text{Ca}_v2.2$  global KO mice significantly reduced capsaicin-induced mechanical hypersensitivity (Fig. 2c,f) suggesting a concentration dependence of IL-1 $\alpha$  for triggering distinct forms of hypersensitivity. Expression levels of IL-1R1 are higher in LTMRs and proprioceptors as compared to *Trpv1*-expressing neurons<sup>75</sup> therefore, it is also possible that *Trpv1*-nociceptors and LTMRs have different sensitivities to IL-1 $\alpha$ .

Others have shown that IL-1R1 receptor activation by IL-1 $\beta$  increases the excitability of cultured neurons isolated from DRG, including via actions on voltage-gated sodium ion channels and potassium channels<sup>48,77,86–88</sup>. As IL-1 $\alpha$  acts through the same IL-1R1 receptor as IL-1 $\beta$ , IL-1 $\alpha$  should have similar biological effects<sup>61,64,66,68</sup>. We confirmed this using calcium imaging and optogenetic stimulation of *Trpv1*-nociceptors. In this platform we show that overnight incubation of IL-1 $\alpha$  increases the responsiveness of cultured *Trpv1*-nociceptors compared to saline-treated control cells (Fig. 4b.) to optical stimulation consistent with other reports using similar methods to assess the actions of proinflammatory cytokines on sensory neurons *ex vivo*<sup>89</sup>. The Wainger lab has previously shown that an increase in the percentage of light sensitive cells as a function of stimulation by blue light reflects increased excitability, as has been observed with potassium channel blockers. Whereas a decrease in the percentage of light sensitive cells as a function of stimulation by blue light reflects decreased excitability, as

shown using voltage-gated sodium and calcium channel blockers<sup>57</sup>. Thus, the percentage of neurons responding to optical stimulation by blue light is increased within this sensitive dynamic range by IL-1 $\alpha$ . Prior studies have implicated phosphorylation, trafficking, and synthesis of new TRPV1 channels in similar sensitization processes by inflammatory mediators<sup>90</sup>, but further studies are needed to better understand the mechanism of how IL-1 $\alpha$  increases neuronal responsiveness. Additional studies are also needed to compare the dose-dependent effects of IL-1 $\alpha$  on *Trpv1*-nociceptors and mechanoreceptors that innervate hind paws<sup>85,91–93</sup>.

In conclusion, we report that IL-1 $\alpha$  is the critical cytokine released from immune cells in skin, underlying rapid, transient, and adaptive neuroinflammation in skin induced by intradermal capsaicin. IL-1 $\alpha$  is necessary and sufficient to couple intense stimulation of *Trpv1* nociceptors to a rapidly developing, but transient, hypersensitivity of local nerve endings in skin to heat and mechanical stimuli. IL-1 $\alpha$  participates in cross-sensitization of neighboring mechanoreceptor nerve endings. The *in vivo* actions and time course of IL-1 $\alpha$  levels in skin, parallel the behavioral responses that define rapid, adaptive neuroinflammation. Our studies provide important insight for the development of more precise therapeutic strategies to target specific phases of the neuroinflammatory response.

## Materials and methods

All mice used were bred at Brown University, and all protocols and procedures were approved by the Brown University Institutional Animal Care and Use Committee (IACUC). All experiments were performed in accordance with approved IACUC protocols and compliance with ARRIVE guidelines. Male and female mice were included in all experiments and were 3–6 months old, unless otherwise specified. Values shown are mean  $\pm$  SE. Experimenters were blind to animal genotype, experimental condition, and solution injected and were only unblinded post analysis, including analysis of interstitial fluid. The  $Ca_v2.2^{-/-}$  global deletion (KO) mouse strain (*Cacna1b*<sup>tm5.1Dil1</sup>, MGI) was generated in our lab by STOP cassette in frame, in exon 1 of *Cacna1b*, as described previously<sup>8</sup>. A wild-type strain was bred in parallel from the same genetic background and used for comparison in some experiments. These wild-type mice were not significantly different in behavioral studies from wild-type littermates and were pooled for analysis. For optogenetic activation of DRG neurons, *Trpv1*-Cre (Jax 017769)<sup>94</sup> male mice were crossed with Ai32(RCL-ChR2(H134R)/EYFP) (Jax 024109)<sup>95</sup> female mice and first-generation *Trpv1*/ChR2-EYFP pups were used for preparation of primary sensory neurons with ChR2-EYFP expressed in *Trpv1*-positive nociceptors.

## Hind paw fluid extraction

Mice were anesthetized using isoflurane (2.0–3.5%) and O<sub>2</sub> (0.6–0.8 LPM) administered continuously via nosecone for the entire fluid extraction process. The plantar surface of the footpad was injected with a 30-gauge insulin needle intradermally in the center of the paw with 50  $\mu$ l of: 0.1% w/v capsaicin, 0.1% w/v capsaicin + 2  $\mu$ M  $\omega$ -conotoxin MVIIA, or 2  $\mu$ M  $\omega$ -conotoxin MVIIA using saline as vehicle in all solutions. For fluid extraction, the same syringe is used to optimize yield. Fluid is collected by slowly drawing back the syringe to pull any free fluid in the subcutaneous pocket. Light pressure is applied to the surrounding area and any leaked fluid on the surface was collected. Typical fluid yield is 7–10  $\mu$ l from two paws per animal and samples from 2 to 4 animals for each condition are pooled into an Eppendorf on dry ice and stored at –80 °C until used for immunoassay analyses.

## Serum isolation

Mice were euthanized with an overdose of isoflurane and cervical dislocation and blood was collected postmortem from the heart via cardiac puncture, samples were pooled from the same animals as their corresponding hind paw fluid samples, and after a 45 min coagulation step, centrifuged at 4 °C for 12 min at 4000 RPM. Serum supernatant was stored at –80 °C for subsequent immunoassays.

## Immunoassays

### *Multiplex bead-based immunoassay (LEGENDplex) fluid analyses*

Custom Mouse Inflammation Panel LEGENDplex (BioLegend, LEGENDplex™) protocol was followed according to the manufacturer's recommendations, and data was acquired using an Attune NxT Flow Cytometer. Pilot hind paw fluid samples from all experimental conditions were collected and used to determine sample dilution factors and to screen for 19 cytokines using capture beads targeting: GM-CSF, IL-1 $\alpha$ , IL-1 $\beta$ , IL-4, IL-6, IL-9, IL-10, IL-12p70, IL-17A, IL-22, IL-23, IL-33, TNF- $\alpha$ , IFN- $\gamma$ , CCL2, CXCL10, CCL4, CCL5, and LIF. We consistently detected only IL-1 $\alpha$  in hind paw fluid in the capsaicin model. After initial screening, we selected 13 cytokines for ongoing analyses based on consistent detection in pilot studies and published literature indicating their potential role in neuroinflammation in skin. Biolegend LEGENDplex Data Analysis Software Suite (Qognit) was used to determine analyte mean fluorescence intensities and calculate concentrations based on concurrently-run standard curves (Supplementary File S3).

### *Electrochemiluminescence spot-based immunoassay fluid validation*

Following LEGENDplex analyses, remaining samples were assayed on two custom Meso Scale Discovery biomarker panels (MSD R-plex: IL-1 $\alpha$ , IL-6; U-plex: TNF $\alpha$ , IL-1 $\beta$ , CCL2, CCL4, CXCL-10, IFN $\gamma$ , IL-33, IL-10, IL-23, MDC). All samples underwent the same freeze–thaw frequency and duration cycles. MSD Biomarker Group 1 (Mouse) protocol was followed according to the manufacturer's recommendations for 96 well plate assays. Plates were read and analyzed using an MESO QuickPlex SQ 120MM instrument. Final concentrations reported were adjusted for sample dilution. The concentration of a particular cytokine was determined using a calibrator standard assayed on each plate (Supplementary File S3).

### Skin explant conditioned media preparation

In anesthetized mice ( $n = 6$ ), we injected capsaicin in one paw, and saline in the contralateral paw prior to skin removal. Mice were euthanized using an overdose of isoflurane followed by cervical dislocation. 5 min post injection and skin was removed from hind paws using 3.5 mm punch biopsy tools (MedBlade, 2 punches/paw). Skin from saline injected-contralateral and capsaicin injected-ipsilateral paws were incubated separately in 600  $\mu\text{l}$  of prewarmed 37 °C RPMI 1610 culture media in 12 well plates. Samples were agitated for 5 min at 250 RPM on an orbital shaker, then 200  $\mu\text{l}$  of conditioned media was removed for analysis. Conditioned media was run in duplicate using an IL-1 $\alpha$  ELISA (ELISA MAX Deluxe Set Mouse IL-1 $\alpha$ , BioLegend Catalog # 433404).

### Behavioral assessments

Radiant heat responses were assessed using Hargreaves (Plantar Analgesia Meter IITC Life Science). Mice were placed in Plexiglas boxes on an elevated glass plate and allowed to habituate for 30 min prior to testing. A radiant heat source was positioned beneath the mice and aimed using low-intensity visible light to the plantar surface of the hind paw. For all trials, laser settings were: Idle intensity at 5% and active intensity at 50% of maximum. Cut off time = 30 s. Trials began once the high-intensity light source was activated and ended once the mouse withdrew, shook, and/or licked their hind paw following stimulation. Immediately upon meeting response criteria, the high-intensity light-source was turned off. The response latency was measured to the nearest 0.01 s for each trial using the built-in timer corresponding to the duration of the high-intensity beam. Three trials were conducted on each hind paw for each mouse, with at least 1 min rest between trials<sup>96</sup>. The average of 3 trials was used for the analysis. N values reported are the number of mice. After baseline measures, mice were anesthetized with isoflurane during all intradermal injections.

Mechanical responses were elicited by an automated Von Frey Plantar Aesthesiometer (catalog #37550, Ugo Basile). Mice were placed in an elevated Plexiglas box with a wire mesh bottom and were allowed to habituate for 30 min prior to testing. The plantar surface of hind paws was assessed using a steady ramp of force ranging from 0 to 8 g for up to 90 s. The trial is automatically terminated when the filament buckles or the paw is withdrawn, force and reaction time are captured. After baseline measures, mice were anesthetized with isoflurane during all intradermal injections.

### Primary DRG harvesting and culture

For optogenetic calcium imaging experiments, male and female mice (C57Bl6/J) between 14 and 21 days old were used. *Trpv1/ChR2-EYFP* strains were generated by crossing *Trpv1-Cre* (Jax 017769) male mice with *LSL-ChR2-EYFP* (Jax 024109) female mice. C1-L6 dorsal root ganglia (DRG) were dissected from isolated and bisected spinal columns of postmortem mice. DRG were placed in cold DMEM/F-12 media (Thermo Fisher 11320033) and transferred to collagenase/dispase for 60 min at 37 °C. To dissociate cells, a series of mechanical trituration steps were performed. Cells were filtered through a strainer, centrifuged using a BSA gradient to separate out debris, and plated on a poly-D-lysine (PDL)/laminin treated 96-well plate. All primary sensory neurons were imaged after being cultured overnight in neurobasal media (Thermo Fisher 211 03049) supplemented with B27 (Thermo Fisher 17504044), Glutamax (Thermo Fisher 35050061), and Penicillin–Streptomycin (Thermo Fisher 15070063).

### Calcium imaging assay

Calcium imaging experiments were performed using an ImageXPress micro confocal high content imaging system (Molecular Devices). Cells were incubated with CalBryte-630AM (AAT Bioquest 20,720, 3  $\mu\text{g}/\text{mL}$  in 0.3% DMSO) calcium indicator for 30 min in the dark. Media was then replaced with 100  $\mu\text{L}$  physiological saline (in mM: 140 NaCl, 5 KCl, 2  $\text{CaCl}_2$ , 1  $\text{MgCl}_2$ , 10 D-glucose, 10 HEPES, and pH 7.3–7.4 with NaOH) immediately prior to cell imaging. For optogenetics experiments, three trains of blue light pulses (1, 5, and 10 pulses per train; 1 ms each at 50 Hz) were delivered and cells were imaged using the APPOINT calcium imaging assay, as described previously<sup>57</sup>.

### Data quantification and statistical analysis

Initial identification and quantification of CalBryte-630AM intensity was performed using a custom journal in ImageXPress (Molecular Devices) analysis software. Briefly, CalBryte-positive cells in each well were identified using a minimum projection of the timelapse image stack based on size and CalBryte intensity. Each cell automatically generated an individual ROI, which was transferred back to the original timelapse stack and the mean intensity of each ROI was calculated for every image. Analysis of cell intensity and quantification was performed in R (Version 4.3.1). Statistical analyses were performed using RStudio (Posit Software), Prism (Version 10; GraphPad), or Excel (Microsoft). All data are presented as the mean  $\pm$  SE. The significance of optical rheobase assay was assessed using two-way ANOVA followed up by Bonferroni's multiple comparisons.

### Data availability

The  $\text{Ca}_v2.2^{-/-}$  mouse strain (*Cacna1b*<sup>tm5.1Dili</sup>) is described in the MGI database and available by request to Diane Lipscombe. All datasets are available by request to Diane Lipscombe.

Received: 18 December 2023; Accepted: 10 April 2024

Published online: 20 April 2024

## References

- Jain, A., Hakim, S. & Woolf, C. J. Unraveling the plastic peripheral neuroimmune interactome. *J. Immunol.* **204**, 257–263. <https://doi.org/10.4049/jimmunol.1900818> (2020).
- Ji, R. R., Nackley, A., Huh, Y., Terrando, N. & Maixner, W. Neuroinflammation and central sensitization in chronic and widespread pain. *Anesthesiology* **129**, 343–366. <https://doi.org/10.1097/ALN.0000000000002130> (2018).
- Cook, S. P. & McCleskey, E. W. Cell damage excites nociceptors through release of cytosolic ATP. *Pain* **95**, 41–47. [https://doi.org/10.1016/s0304-3959\(01\)00372-4](https://doi.org/10.1016/s0304-3959(01)00372-4) (2002).
- Costigan, M., Scholz, J. & Woolf, C. J. Neuropathic pain: A maladaptive response of the nervous system to damage. *Annu. Rev. Neurosci.* **32**, 1–32. <https://doi.org/10.1146/annurev.neuro.051508.135531> (2009).
- Scholz, J. & Woolf, C. J. Can we conquer pain?. *Nat. Neurosci.* **5**(Suppl), 1062–1067 (2002).
- Costigan, M. & Woolf, C. Pain: Molecular mechanisms. *J. Pain* **1**, 35–44 (2000).
- Louis, S. M., Jamieson, A., Russell, N. J. & Dockray, G. J. The role of substance P and calcitonin gene-related peptide in neurogenic plasma extravasation and vasodilatation in the rat. *Neuroscience* **32**, 581–586. [https://doi.org/10.1016/0306-4522\(89\)90281-9](https://doi.org/10.1016/0306-4522(89)90281-9) (1989).
- DuBreuil, D. M. *et al.* Heat But not mechanical hypersensitivity depends on voltage-gated CaV2.2 calcium channel activity in peripheral axon terminals innervating skin. *J. Neurosci.* **41**, 7546–7560. <https://doi.org/10.1523/JNEUROSCI.0195-21.2021> (2021).
- Chi, X. X. *et al.* Regulation of N-type voltage-gated calcium channels (Cav2.2) and transmitter release by collapsin response mediator protein-2 (CRMP-2) in sensory neurons. *J. Cell Sci.* **122**, 4351–4362. <https://doi.org/10.1242/jcs.053280> (2009).
- Chai, Z. *et al.* CaV2.2 gates calcium-independent but voltage-dependent secretion in mammalian sensory neurons. *Neuron* **96**, 1317–1326e1314. <https://doi.org/10.1016/j.neuron.2017.10.028> (2017).
- Duan, J. H., Hodgson, K. E., Hingtgen, C. M. & Nicol, G. D. N-type calcium current, Cav2.2, is enhanced in small-diameter sensory neurons isolated from Nf1+/- mice. *Neuroscience* **270**, 192–202. <https://doi.org/10.1016/j.neuroscience.2014.04.021> (2014).
- McCleskey, E. W. *et al.* Omega-conotoxin: Direct and persistent blockade of specific types of calcium channels in neurons but not muscle. *Proc. Natl. Acad. Sci. U. S. A.* **84**, 4327–4331. <https://doi.org/10.1073/pnas.84.12.4327> (1987).
- Altier, C. *et al.* Differential role of N-type calcium channel splice isoforms in pain. *J. Neurosci.* **27**, 6363–6373. <https://doi.org/10.1523/JNEUROSCI.0307-07.2007> (2007).
- Andrade, A., Denome, S., Jiang, Y. Q., Marangoudakis, S. & Lipscombe, D. Opioid inhibition of N-type Ca<sup>2+</sup> channels and spinal analgesia couple to alternative splicing. *Nat. Neurosci.* **13**, 1249–1256. <https://doi.org/10.1038/nn.2643> (2010).
- Snutch, T. P. Targeting chronic and neuropathic pain: The N-type calcium channel comes of age. *NeuroRx* **2**, 662–670. <https://doi.org/10.1602/neurorx.2.4.662> (2005).
- Altier, C. & Zamponi, G. W. Targeting Ca<sup>2+</sup> channels to treat pain: T-type versus N-type. *Trends Pharmacol. Sci.* **25**, 465–470. <https://doi.org/10.1016/j.tips.2004.07.004> (2004).
- Gerovich, Z. *et al.* Inhibition of N-type voltage-activated calcium channels in rat dorsal root ganglion neurons by P2Y receptors is a possible mechanism of ADP-induced analgesia. *J. Neurosci.* **24**, 797–807. <https://doi.org/10.1523/JNEUROSCI.4019-03.2004> (2004).
- Callaghan, B. *et al.* Analgesic alpha-conotoxins Vc1.1 and Rg1A inhibit N-type calcium channels in rat sensory neurons via GABAB receptor activation. *J. Neurosci.* **28**, 10943–10951. <https://doi.org/10.1523/JNEUROSCI.3594-08.2008> (2008).
- Pitake, S., Middleton, L. J., Abdus-Saboor, I. & Mishra, S. K. Inflammation induced sensory nerve growth and pain hypersensitivity requires the N-type calcium channel Cav2.2. *Front. Neurosci.* **13**, 1009. <https://doi.org/10.3389/fnins.2019.01009> (2019).
- Murali, S. S. *et al.* High-voltage-activated calcium current subtypes in mouse DRG neurons adapt in a subpopulation-specific manner after nerve injury. *J. Neurophysiol.* **113**, 1511–1519. <https://doi.org/10.1152/jn.00608.2014> (2015).
- Ramgoolam, K. H. & Dolphin, A. C. Capsaicin-induced endocytosis of endogenous presynaptic Ca(V)2.2 in DRG-spinal cord co-cultures inhibits presynaptic function. *Function (Oxf)* **4**, zqac058. <https://doi.org/10.1093/function/zqac058> (2023).
- Lipscombe, D., Allen, S. E. & Toro, C. P. Control of neuronal voltage-gated calcium ion channels from RNA to protein. *Trends Neurosci.* **36**, 598–609. <https://doi.org/10.1016/j.tins.2013.06.008> (2013).
- Timmermann, D. B., Westenbroek, R. E., Schousboe, A. & Catterall, W. A. Distribution of high-voltage-activated calcium channels in cultured gamma-aminobutyric acidergic neurons from mouse cerebral cortex. *J. Neurosci. Res.* **67**, 48–61. <https://doi.org/10.1002/jnr.10074> (2002).
- Westenbroek, R. E. *et al.* Biochemical properties and subcellular distribution of an N-type calcium channel alpha 1 subunit. *Neuron* **9**, 1099–1115. [https://doi.org/10.1016/0896-6273\(92\)90069-p](https://doi.org/10.1016/0896-6273(92)90069-p) (1992).
- Dunlap, K., Luebke, J. I. & Turner, T. J. Identification of calcium channels that control neurosecretion. *Science* **266**, 828–831 (1994).
- Filloux, F., Schapper, A., Naisbitt, S. R., Olivera, B. M. & McIntosh, J. M. Complex patterns of [125I]omega-conotoxin GVIA binding site expression during postnatal rat brain development. *Brain Res. Dev. Brain Res.* **78**, 131–136. [https://doi.org/10.1016/0165-3806\(94\)90017-5](https://doi.org/10.1016/0165-3806(94)90017-5) (1994).
- Miljanich, G. P. & Ramachandran, J. Antagonists of neuronal calcium channels: Structure, function, and therapeutic implications. *Annu. Rev. Pharmacol. Toxicol.* **35**, 707–734. <https://doi.org/10.1146/annurev.pa.35.040195.003423> (1995).
- Heinke, B., Balzer, E. & Sandkuhler, J. Pre- and postsynaptic contributions of voltage-evoked Ca<sup>2+</sup> channels to nociceptive transmission in rat spinal lamina I neurons. *Eur. J. Neurosci.* **19**, 103–111. <https://doi.org/10.1046/j.1460-9568.2003.03083.x> (2004).
- Heinke, B., Gingl, E. & Sandkuhler, J. Multiple targets of mu-opioid receptor-mediated presynaptic inhibition at primary afferent Delta- and C-fibers. *J. Neurosci.* **31**, 1313–1322. <https://doi.org/10.1523/JNEUROSCI.4060-10.2011> (2011).
- Jayamane, A. *et al.* Spinal actions of omega-conotoxins, CVID, MVIIA and related peptides in a rat neuropathic pain model. *Br. J. Pharmacol.* **170**, 245–254. <https://doi.org/10.1111/bph.12251> (2013).
- Motin, L. & Adams, D. J. Omega-Conotoxin inhibition of excitatory synaptic transmission evoked by dorsal root stimulation in rat superficial dorsal horn. *Neuropharmacology* **55**, 860–864. <https://doi.org/10.1016/j.neuropharm.2008.06.049> (2008).
- Bowersox, S. S. *et al.* Selective N-type neuronal voltage-sensitive calcium channel blocker, SNX-111, produces spinal antinociception in rat models of acute, persistent and neuropathic pain. *J. Pharmacol. Exp. Ther.* **279**, 1243–1249 (1996).
- Wang, Y. X. *et al.* Peripheral versus central potencies of N-type voltage-sensitive calcium channel blockers. *Naunyn Schmiedeberg's Arch. Pharmacol.* **357**, 159–168. <https://doi.org/10.1007/pl00005150> (1998).
- Atanassoff, P. G. *et al.* Ziconotide, a new N-type calcium channel blocker, administered intrathecally for acute postoperative pain. *Reg. Anesth. Pain Med.* **25**, 274–278. [https://doi.org/10.1016/s1098-7339\(00\)90010-5](https://doi.org/10.1016/s1098-7339(00)90010-5) (2000).
- Wang, Y. X., Pettus, M., Gao, D., Phillips, C. & Scott Bowersox, S. Effects of intrathecal administration of ziconotide, a selective neuronal N-type calcium channel blocker, on mechanical allodynia and heat hyperalgesia in a rat model of postoperative pain. *Pain* **84**, 151–158. [https://doi.org/10.1016/s0304-3959\(99\)00197-9](https://doi.org/10.1016/s0304-3959(99)00197-9) (2000).
- Scott, D. A., Wright, C. E. & Angus, J. A. Actions of intrathecal omega-conotoxins CVID, GVIA, MVIIA, and morphine in acute and neuropathic pain in the rat. *Eur. J. Pharmacol.* **451**, 279–286. [https://doi.org/10.1016/s0014-2999\(02\)02247-1](https://doi.org/10.1016/s0014-2999(02)02247-1) (2002).
- Wermeling, D. P. Ziconotide, an intrathecally administered N-type calcium channel antagonist for the treatment of chronic pain. *Pharmacotherapy* **25**, 1084–1094. <https://doi.org/10.1592/phco.2005.25.8.1084> (2005).
- McGovern, J. G. Targeting N-type and T-type calcium channels for the treatment of pain. *Drug Discov. Today* **11**, 245–253. [https://doi.org/10.1016/S1359-6446\(05\)03662-7](https://doi.org/10.1016/S1359-6446(05)03662-7) (2006).

39. Schroeder, C. I., Doering, C. J., Zamponi, G. W. & Lewis, R. J. N-type calcium channel blockers: novel therapeutics for the treatment of pain. *Med. Chem.* **2**, 535–543. <https://doi.org/10.2174/157340606778250216> (2006).
40. Jiang, Y. Q., Andrade, A. & Lipscombe, D. Spinal morphine but not ziconotide or gabapentin analgesia is affected by alternative splicing of voltage-gated calcium channel CaV2.2 pre-mRNA. *Mol. Pain* **9**, 67. <https://doi.org/10.1186/1744-8069-9-67> (2013).
41. Khanna, R. *et al.* Targeting the CaV $\alpha$ -CaV $\beta$  interaction yields an antagonist of the N-type CaV2.2 channel with broad antinociceptive efficacy. *Pain* **160**, 1644–1661. <https://doi.org/10.1097/j.pain.0000000000001524> (2019).
42. Miljanich, G. P. Ziconotide: Neuronal calcium channel blocker for treating severe chronic pain. *Curr. Med. Chem.* **11**, 3029–3040. <https://doi.org/10.2174/0929867043363884> (2004).
43. Staats, P. S. *et al.* Intrathecal ziconotide in the treatment of refractory pain in patients with cancer or AIDS: A randomized controlled trial. *JAMA* **291**, 63–70. <https://doi.org/10.1001/jama.291.1.63> (2004).
44. Giuliani, A. L., Sarti, A. C., Falzoni, S. & Di Virgilio, F. The P2X7 Receptor-Interleukin-1 Liaison. *Front. Pharmacol.* **8**, 123. <https://doi.org/10.3389/fphar.2017.00123> (2017).
45. Pinho-Ribeiro, F. A., Verri, W. A. Jr. & Chiu, I. M. Nociceptor sensory neuron-immune interactions in pain and inflammation. *Trends Immunol.* **38**, 5–19. <https://doi.org/10.1016/j.it.2016.10.001> (2017).
46. Tamari, M., Ver Heul, A. M. & Kim, B. S. Immunosenescence: Neuroimmune cross talk in the skin. *Annu. Rev. Immunol.* **39**, 369–393. <https://doi.org/10.1146/annurev-immunol-101719-113805> (2021).
47. Trier, A. M., Mack, M. R. & Kim, B. S. The neuroimmune axis in skin sensation, inflammation, and immunity. *J. Immunol.* **202**, 2829–2835. <https://doi.org/10.4049/jimmunol.1801473> (2019).
48. Binshtok, A. M. *et al.* Nociceptors are interleukin-1 $\beta$  sensors. *J. Neurosci.* **28**, 14062–14073. <https://doi.org/10.1523/JNEUROSCI.3795-08.2008> (2008).
49. Summer, G. J. *et al.* Proinflammatory cytokines mediating burn-injury pain. *Pain* **135**, 98–107. <https://doi.org/10.1016/j.pain.2007.05.012> (2008).
50. Miller, R. J., Jung, H., Bhangoo, S. K. & White, F. A. Cytokine and chemokine regulation of sensory neuron function. *Handb. Exp. Pharmacol.* [https://doi.org/10.1007/978-3-540-79090-7\\_12](https://doi.org/10.1007/978-3-540-79090-7_12) (2009).
51. Baumann, T. K., Simone, D. A., Shain, C. N. & LaMotte, R. H. Neurogenic hyperalgesia: the search for the primary cutaneous afferent fibers that contribute to capsaicin-induced pain and hyperalgesia. *J. Neurophysiol.* **66**, 212–227. <https://doi.org/10.1152/jn.1991.66.1.212> (1991).
52. Gilchrist, H. D., Allard, B. L. & Simone, D. A. Enhanced withdrawal responses to heat and mechanical stimuli following intraplantar injection of capsaicin in rats. *Pain* **67**, 179–188. [https://doi.org/10.1016/0304-3959\(96\)03104-1](https://doi.org/10.1016/0304-3959(96)03104-1) (1996).
53. Simone, D. A., Baumann, T. K. & LaMotte, R. H. Dose-dependent pain and mechanical hyperalgesia in humans after intradermal injection of capsaicin. *Pain* **38**, 99–107. [https://doi.org/10.1016/0304-3959\(89\)90079-1](https://doi.org/10.1016/0304-3959(89)90079-1) (1989).
54. Bowersox, S., Mandema, J., Tarczy-Hornoch, K., Miljanich, G. & Luther, R. R. Pharmacokinetics of SNX-111, a selective N-type calcium channel blocker, in rats and cynomolgus monkeys. *Drug Metab. Dispos.* **25**, 379–383 (1997).
55. White, D. M. & Cousins, M. J. Effect of subcutaneous administration of calcium channel blockers on nerve injury-induced hyperalgesia. *Brain Res.* **801**, 50–58. [https://doi.org/10.1016/s0006-8993\(98\)00539-3](https://doi.org/10.1016/s0006-8993(98)00539-3) (1998).
56. Xiao, W. H. & Bennett, G. J. Synthetic omega-conopeptides applied to the site of nerve injury suppress neuropathic pains in rats. *J. Pharmacol. Exp. Ther.* **274**, 666–672 (1995).
57. DuBreuil, D. M. *et al.* A high-content platform for physiological profiling and unbiased classification of individual neurons. *Cell Rep. Methods* <https://doi.org/10.1016/j.crmeth.2021.100004> (2021).
58. Sandkuhler, J. Models and mechanisms of hyperalgesia and allodynia. *Physiol. Rev.* **89**, 707–758. <https://doi.org/10.1152/physrev.00025.2008> (2009).
59. Liu, M., Max, M. B., Robinovitz, E., Gracely, R. H. & Bennett, G. J. The human capsaicin model of allodynia and hyperalgesia: Sources of variability and methods for reduction. *J. Pain Symptom Manage.* **16**, 10–20. [https://doi.org/10.1016/s0885-3924\(98\)00026-8](https://doi.org/10.1016/s0885-3924(98)00026-8) (1998).
60. Stenina, M. A. *et al.* Cytokine profile of the blood in mice with normal and abnormal heart rhythm. *Bull. Exp. Biol. Med.* **152**, 692–695. <https://doi.org/10.1007/s10517-012-1608-9> (2012).
61. Rider, P., Voronov, E., Dinarello, C. A., Apte, R. N. & Cohen, I. Alarmins: Feel the stress. *J. Immunol.* **198**, 1395–1402. <https://doi.org/10.4049/jimmunol.1601342> (2017).
62. Li, Y. *et al.* Cytokine patterns in the blister fluid and plasma of patients with fracture blisters. *Int. Immunopharmacol.* **123**, 110738. <https://doi.org/10.1016/j.intimp.2023.110738> (2023).
63. Sjobom, U., Christenson, K., Hellstrom, A. & Nilsson, A. K. Inflammatory markers in suction blister fluid: A comparative study between interstitial fluid and plasma. *Front. Immunol.* **11**, 597632. <https://doi.org/10.3389/fimmu.2020.597632> (2020).
64. Cavalli, G. *et al.* Interleukin 1 $\alpha$ : A comprehensive review on the role of IL-1 $\alpha$  in the pathogenesis and treatment of autoimmune and inflammatory diseases. *Autoimmun. Rev.* **20**, 102763. <https://doi.org/10.1016/j.autrev.2021.102763> (2021).
65. Werman, A. *et al.* The precursor form of IL-1 $\alpha$  is an intracrine proinflammatory activator of transcription. *Proc. Natl. Acad. Sci. U. S. A.* **101**, 2434–2439. <https://doi.org/10.1073/pnas.0308705101> (2004).
66. Dinarello, C. A. Overview of the IL-1 family in innate inflammation and acquired immunity. *Immunol. Rev.* **281**, 8–27. <https://doi.org/10.1111/imr.12621> (2018).
67. Lonnemann, G. *et al.* Differences in the synthesis and kinetics of release of interleukin 1 $\alpha$ , interleukin 1 $\beta$  and tumor necrosis factor from human mononuclear cells. *Eur. J. Immunol.* **19**, 1531–1536. <https://doi.org/10.1002/eji.1830190903> (1989).
68. Mantovani, A., Dinarello, C. A., Molgora, M. & Garlanda, C. Interleukin-1 and related cytokines in the regulation of inflammation and immunity. *Immunity* **50**, 778–795. <https://doi.org/10.1016/j.immuni.2019.03.012> (2019).
69. Martin, P., Goldstein, J. D., Mermoud, L., Diaz-Barreiro, A. & Palmer, G. IL-1 family antagonists in mouse and human skin inflammation. *Front. Immunol.* **12**, 652846. <https://doi.org/10.3389/fimmu.2021.652846> (2021).
70. Hung, A. L., Lim, M. & Doshi, T. L. Targeting cytokines for treatment of neuropathic pain. *Scand. J. Pain* **17**, 287–293. <https://doi.org/10.1016/j.sjpain.2017.08.002> (2017).
71. Vanderwall, A. G. & Milligan, E. D. Cytokines in pain: Harnessing endogenous anti-inflammatory signaling for improved pain management. *Front. Immunol.* **10**, 3009. <https://doi.org/10.3389/fimmu.2019.03009> (2019).
72. Scholz, J. & Woolf, C. J. The neuropathic pain triad: Neurons, immune cells and glia. *Nat. Neurosci.* **10**, 1361–1368. <https://doi.org/10.1038/nn1992> (2007).
73. Huntula, S., Saegusa, H., Wang, X., Zong, S. & Tanabe, T. Involvement of N-type Ca<sup>2+</sup> channel in microglial activation and its implications to aging-induced exaggerated cytokine response. *Cell Calcium* **82**, 102059. <https://doi.org/10.1016/j.ceca.2019.102059> (2019).
74. Saegusa, H. *et al.* Suppression of inflammatory and neuropathic pain symptoms in mice lacking the N-type Ca<sup>2+</sup> channel. *EMBO J.* **20**, 2349–2356. <https://doi.org/10.1093/emboj/20.10.2349> (2001).
75. Sharma, N. *et al.* The emergence of transcriptional identity in somatosensory neurons. *Nature* **577**, 392–398. <https://doi.org/10.1038/s41586-019-1900-1> (2020).
76. Cai, S., Gomez, K., Moutal, A. & Khanna, R. Targeting T-type/CaV3.2 channels for chronic pain. *Transl. Res.* **234**, 20–30. <https://doi.org/10.1016/j.trsl.2021.01.002> (2021).
77. Stemkowski, P. L. *et al.* Identification of interleukin-1 $\beta$  as a key mediator in the upregulation of Cav3.2-USP5 interactions in the pain pathway. *Mol. Pain* **13**, 1744806917724698. <https://doi.org/10.1177/1744806917724698> (2017).

78. Picard, E. *et al.* Role of T CD4(+) cells, macrophages, C-low threshold mechanoreceptors and spinal Ca(v) 3.2 channels in inflammation and related pain-like symptoms in murine inflammatory models. *Br. J. Pharmacol.* **180**, 385–400. <https://doi.org/10.1111/bph.15956> (2023).
79. Bodo, E. *et al.* A hot new twist to hair biology: Involvement of vanilloid receptor-1 (VR1/TRPV1) signaling in human hair growth control. *Am. J. Pathol.* **166**, 985–998. [https://doi.org/10.1016/S0002-9440\(10\)62320-6](https://doi.org/10.1016/S0002-9440(10)62320-6) (2005).
80. Bertin, S. *et al.* The ion channel TRPV1 regulates the activation and proinflammatory properties of CD4(+) T cells. *Nat. Immunol.* **15**, 1055–1063. <https://doi.org/10.1038/ni.3009> (2014).
81. Mariotton, J. *et al.* TRPV1 activation in human Langerhans cells and T cells inhibits mucosal HIV-1 infection via CGRP-dependent and independent mechanisms. *Proc. Natl. Acad. Sci. U. S. A.* **120**, e2302509120. <https://doi.org/10.1073/pnas.2302509120> (2023).
82. Culp, W. J., Ochoa, J., Cline, M. & Dotson, R. Heat and mechanical hyperalgesia induced by capsaicin. Cross modality threshold modulation in human C nociceptors. *Brain* **112**(Pt 5), 1317–1331. <https://doi.org/10.1093/brain/112.5.1317> (1989).
83. Magerl, W., Fuchs, P. N., Meyer, R. A. & Treede, R. D. Roles of capsaicin-insensitive nociceptors in cutaneous pain and secondary hyperalgesia. *Brain* **124**, 1754–1764. <https://doi.org/10.1093/brain/124.9.1754> (2001).
84. Szolcsanyi, J., Anton, F., Reeh, P. W. & Handwerker, H. O. Selective excitation by capsaicin of mechano-heat sensitive nociceptors in rat skin. *Brain Res.* **446**, 262–268. [https://doi.org/10.1016/0006-8993\(88\)90885-2](https://doi.org/10.1016/0006-8993(88)90885-2) (1988).
85. Koltzenburg, M., Stucky, C. L. & Lewin, G. R. Receptive properties of mouse sensory neurons innervating hairy skin. *J. Neurophysiol.* **78**, 1841–1850. <https://doi.org/10.1152/jn.1997.78.4.1841> (1997).
86. Stembkowski, P. L., Noh, M. C., Chen, Y. & Smith, P. A. Increased excitability of medium-sized dorsal root ganglion neurons by prolonged interleukin-1beta exposure is K(+) channel dependent and reversible. *J. Physiol.* **593**, 3739–3755. <https://doi.org/10.1113/JP270905> (2015).
87. Stembkowski, P. L. & Smith, P. A. Long-term IL-1beta exposure causes subpopulation-dependent alterations in rat dorsal root ganglion neuron excitability. *J. Neurophysiol.* **107**, 1586–1597. <https://doi.org/10.1152/jn.00587.2011> (2012).
88. von Banchet, G. S. *et al.* Molecular effects of interleukin-1beta on dorsal root ganglion neurons: Prevention of ligand-induced internalization of the bradykinin 2 receptor and downregulation of G protein-coupled receptor kinase 2. *Mol. Cell. Neurosci.* **46**, 262–271. <https://doi.org/10.1016/j.mcn.2010.09.009> (2011).
89. Prado, J. *et al.* Cytokine receptor clustering in sensory neurons with an engineered cytokine fusion protein triggers unique pain resolution pathways. *Proc. Natl. Acad. Sci. U. S. A.* <https://doi.org/10.1073/pnas.2009647118> (2021).
90. Hucho, T. & Levine, J. D. Signaling pathways in sensitization: Toward a nociceptor cell biology. *Neuron* **55**, 365–376. <https://doi.org/10.1016/j.neuron.2007.07.008> (2007).
91. Beaudry, H., Daou, I., Ase, A. R., Ribeiro-da-Silva, A. & Seguela, P. Distinct behavioral responses evoked by selective optogenetic stimulation of the major TRPV1+ and MrgD+ subsets of C-fibers. *Pain* **158**, 2329–2339. <https://doi.org/10.1097/j.pain.0000000000001016> (2017).
92. Li, L. *et al.* The functional organization of cutaneous low-threshold mechanosensory neurons. *Cell* **147**, 1615–1627. <https://doi.org/10.1016/j.cell.2011.11.027> (2011).
93. Barabas, M. E. & Stucky, C. L. TRPV1, but not TRPA1, in primary sensory neurons contributes to cutaneous incision-mediated hypersensitivity. *Mol. Pain* **9**, 9. <https://doi.org/10.1186/1744-8069-9-9> (2013).
94. Cavanaugh, D. J. *et al.* Trpv1 reporter mice reveal highly restricted brain distribution and functional expression in arteriolar smooth muscle cells. *J. Neurosci.* **31**, 5067–5077. <https://doi.org/10.1523/JNEUROSCI.6451-10.2011> (2011).
95. Madisen, L. *et al.* A toolbox of Cre-dependent optogenetic transgenic mice for light-induced activation and silencing. *Nat. Neurosci.* **15**, 793–802. <https://doi.org/10.1038/nn.3078> (2012).
96. Hargreaves, K., Dubner, R., Brown, F., Flores, C. & Joris, J. A new and sensitive method for measuring thermal nociception in cutaneous hyperalgesia. *Pain* **32**, 77–88. [https://doi.org/10.1016/0304-3959\(88\)90026-7](https://doi.org/10.1016/0304-3959(88)90026-7) (1988).
97. Walcher, J. *et al.* Specialized mechanoreceptor systems in rodent glabrous skin. *J. Physiol.* **596**, 4995–5016. <https://doi.org/10.1113/JP276608> (2018).

## Author contributions

A-M.N.S, M.J.C, S.H.L, B.J.W, A.M.J and D.L. contributed to research design; A-M.N.S, M.J.C, and S.H.L performed research experiments; A-M.N.S, M.J.C, S.H.L, and D.L. analyzed data; A-M.N.S and D.L. wrote the manuscript. All authors reviewed the manuscript.

## Funding

This work was supported by NINDS NS055251 (D.L.); NIH IMSD R25GM083270 (A-M.N.S); NHLBI R01HL165259 (A.M.J.), NHLBI R01HL126887 (A.M.J.), P20GM121344 Pilot Project (A.M.J.), Carney Innovation Award (A.M.J.); NIA 5R21AG075419 (B.J.W.).

## Competing interests

The authors declare no competing interests.

## Additional information

**Supplementary Information** The online version contains supplementary material available at <https://doi.org/10.1038/s41598-024-59424-6>.

**Correspondence** and requests for materials should be addressed to D.L.

**Reprints and permissions information** is available at [www.nature.com/reprints](http://www.nature.com/reprints).

**Publisher's note** Springer Nature remains neutral with regard to jurisdictional claims in published maps and institutional affiliations.



**Open Access** This article is licensed under a Creative Commons Attribution 4.0 International License, which permits use, sharing, adaptation, distribution and reproduction in any medium or format, as long as you give appropriate credit to the original author(s) and the source, provide a link to the Creative Commons licence, and indicate if changes were made. The images or other third party material in this article are included in the article's Creative Commons licence, unless indicated otherwise in a credit line to the material. If material is not included in the article's Creative Commons licence and your intended use is not permitted by statutory regulation or exceeds the permitted use, you will need to obtain permission directly from the copyright holder. To view a copy of this licence, visit <http://creativecommons.org/licenses/by/4.0/>.

© The Author(s) 2024